

Quasi-one-dimensional pyroxene $\text{NaFeGe}_2\text{O}_6$: the magnetic structure and magnetic phase diagram

T. Drokina, G. Petrakovskii, L. Keller, J. Schefer

We present the additional results of neutron diffraction measurements on $\text{NaFe}^{3+}\text{Ge}_2\text{O}_6$. The temperature dependence of the $\text{NaFeGe}_2\text{O}_6$ specific heat in the absence of the external magnetic field ($H = 0$) exhibits a sharp maxima at the temperatures $T_1 = 11.6$ K and $T_2 = 13$ K. The results of neutron diffraction are confirmed the existing two magnetic phases in zero magnetic field. In this compound there is antiferromagnetic long-range order, Neel temperature $T_N = 13$ K. The iron-containing pyroxene neutron diffraction data indicate the incommensurate magnetic structure at the temperatures 1.6 – 11.5 K. It consists of antiferromagnetically coupled a pairs of the Fe^{3+} spins with helical modulation within the a - c plane of the crystal lattice. The magnetic structure is unclear at the temperature range $11.5 \text{ K} > T > 13 \text{ K}$.

Keywords: pyroxene $\text{NaFeGe}_2\text{O}_6$, incommensurate magnetic structure, magnetic phase diagram, neutron scattering.

Представлены результаты дополнительного исследования соединения $\text{NaFe}^{3+}\text{Ge}_2\text{O}_6$ методом упругого рассеяния нейтронов. Исследование температурной зависимости теплоемкости в отсутствие внешнего магнитного поля показало наличие двух фазовых переходов при температурах $T_1 = 11.5$ К и $T_2 = 13$ К. Изучение упругого рассеяния нейтронов подтвердило существование двух магнитных фазовых переходов в нулевом магнитном поле. В соединении $\text{NaFeGe}_2\text{O}_6$ имеет место переход из парамагнитного состояния в упорядоченное при $T_N = 13$ К. При температуре $T_c = 11.5$ К образец подвергается дополнительному фазовому переходу в состояние с несоизмеримой магнитной структурой, представляющей собой антиферромагнитную спираль, сформированную из пар спинов ионов Fe^{3+} с геликоидальной модуляцией в плоскости a - c кристаллической решетки. Магнитная структура соединения не известна в температурном диапазоне $11.5 \text{ K} > T > 13 \text{ K}$.

Ключевые слова: пироксен $\text{NaFeGe}_2\text{O}_6$, несопротивимая магнитная структура, магнитная фазовая диаграмма, нейтронное рассеяние

Introduction

Pyroxenes are formed a broad class of materials for physical investigations. The pyroxenes compounds have a chemical formula ABX_2O_6 ($\text{A} = \text{Na}, \text{Li}$ and Ca ; $\text{B} = \text{Mg}, \text{Cr}, \text{Cu}, \text{Ni}, \text{Fe}$, etc.; $\text{X} = \text{Ge}, \text{Si}$). If the A position is occupied by the monovalent cations (Na, Li), B adopts attitude of the trivalent metals (Fe, Cr , etc.). If the A position is occupied by the divalent cation (Ca), in this case B adopts attitude of the divalent cation ($\text{Ni}, \text{Fe}, \text{Co}$, etc.). Some pyroxenes are a rock forming minerals and they have been studied in geosciences. The most of the germanates and silicates (for ex., $\text{NaFe}^{3+}\text{Ge}_2\text{O}_6$, $\text{LiFe}^{3+}\text{Ge}_2\text{O}_6$) are attracted significant interest in solid state physics due to their low dimensional magnetic systems [1,2].

The new interest to these physical systems is appeared in spintronics — new direction in the modern electronics — due to the discovery of the strong interaction between the magnetic and electric subsystems in the compounds $\text{NaFeSi}_2\text{O}_6$, $\text{LiFeSi}_2\text{O}_6$ and $\text{LiCrSi}_2\text{O}_6$ which are formed a new class of multiferroics [3].

The pyroxene-type compounds exhibit a variety of different magnetically ordered states (table 1). The most of them are antiferromagnetic [4 – 16]. There is ferromagnetic (for ex., $\text{NaCr}^{3+}\text{Ge}_2\text{O}_6$) [17 – 19]. Some pyroxene compounds show the orbitally driven spin gap state (for ex., $\text{NaTiSi}_2\text{O}_6$) [21]. The variety of pyroxene magnetic properties are connected with the features of the crystal structure which is allowed the existing of a magnetic frustration.

Table 1

The magnetic states in pyroxenes compounds

Compounds	Magnetically ordered state	References
NaV ³⁺ Ge ₂ O ₆	antiferromagnetic long-range order ($T_N = 22$ K)	[4, 5]
LiV ³⁺ Ge ₂ O ₆	antiferromagnetic long-range order ($T_N = 24$ K)	[4 – 7]
NaV ³⁺ Si ₂ O ₆	antiferromagnetic long-range order ($T_N = 17$ K)	[4]
LiV ³⁺ Si ₂ O ₆	antiferromagnetic long-range order ($T_N = 22$ K)	[4]
LiFe ³⁺ Ge ₂ O ₆	antiferromagnetic long-range order ($T_N = 20$ K)	[8 – 10]
NaFe ³⁺ Ge ₂ O ₆	antiferromagnetic long-range order ($T_N = 13$ K), incommensurate magnetic structure at 1.6 – 11.5 K	[11 – 14]
NaFe ³⁺ Si ₂ O ₆	antiferromagnetic long-range order ($T_N = 5$ K)	[14 – 16]
LiFe ³⁺ Si ₂ O ₆	antiferromagnetic long-range order ($T_N = 18$ K)	[8, 15, 16]
NaCr ³⁺ Ge ₂ O ₆	ferromagnetic long-range order ($T_c = 6$ K)	[17 – 19]
LiCr ³⁺ Ge ₂ O ₆	antiferromagnetic long-range order ($T_N = 4$ K)	[17]
LiCr ³⁺ Si ₂ O ₆	antiferromagnetic long-range order ($T_N = 11$ K)	[17]
NaCr ³⁺ Si ₂ O ₆	antiferromagnetic long-range order ($T_N = 3$ K)	[17, 19, 20]
NaTi ³⁺ Si ₂ O ₆	spin-singlet ground state ($T_c = 210$ K)	[21, 22]
LiTi ³⁺ Si ₂ O ₆	spin-singlet ground state ($T_c = 230$ K)	[21]
CaCu ²⁺ Ge ₂ O ₆	spin-singlet ground state ($T_c = 40$ K)	[23]
CaFe ²⁺ Si ₂ O ₆	antiferromagnetic long-range order ($T_N = 38$ K)	[24, 25]
CaCo ²⁺ Si ₂ O ₆	antiferromagnetic long-range order ($T_N = 10$ K)	[26]
CaNi ²⁺ Si ₂ O ₆	antiferromagnetic long-range order ($T_N = 20$ K)	[26]
CaCo ²⁺ Ge ₂ O ₆	antiferromagnetic long-range order ($T_N = 18$ K)	[25]
CaMn ²⁺ Ge ₂ O ₆	antiferromagnetic long-range order ($T_N = 12$ K)	[25]
CaNi ²⁺ Ge ₂ O ₆	antiferromagnetic long-range order ($T_N = 18$ K)	[25]

We investigated the iron containing metagermanate NaFeGe₂O₆ with clinopyroxene crystal structure (a monoclinic space group C2/c, Z = 4), which was first described at room temperature in [27]. The nuclear structure is remained the same down to 2,5 K [14]. The lattice parameters at room temperature are $a = 10,01$ Å; $b = 8,94$ Å; $c = 5,52$ Å; beta = 108 e [27].

The crystal structure consists of one-dimensional zigzag chains of edge-sharing FeO₆ octahedra which running parallel the crystallographic c axis. The GeO₄ tetrahedra are connected into infinite chains extended along the crystallographic c axis. The two types of chains alternate along the crystallographic b axis.

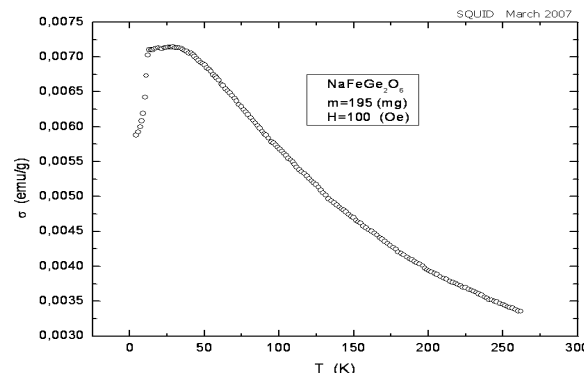


Fig. 1. Temperature dependence of the magnetization in NaFeGe₂O₆.

The magnetism of the pyroxene NaFeGe₂O₆ is determined by spins on Fe³⁺ ions ($S = 5/2$).

We measured the temperature dependence of the magnetization $\sigma(T)$ in magnetic field 0,01 T by a superconducting quantum interference device (SQUID) magnetometer between 4.2 and 300 K [11]. Bulk magnetic measurements of the temperature dependence of the magnetization show a broad maximum near 25 K (fig. 1), which is the characteristic property of low dimensional magnetic spin systems.

In previous papers we found the incommensurate magnetic structure due to the magnetic exchange interactions competitions in the polycrystalline NaFeGe₂O₆ [12, 13]. This result was confirmed on a NaFeGe₂O₆ single crystal [14].

To subsequent study the magnetic phase transitions and the magnetic structure in this compound it has been used the neutron scattering measurements.

Sample preparation and experimental procedure

Polycrystalline NaFeGe₂O₆ was obtained by a solid-state reaction method from the stoichiometric mixture of Na₂CO₃, Fe₂O₃, GeO₂ at the temperatures of 800 – 900 °C in air at four stages each with a duration of 24 h. The sample was free from magnetic impurities, which were not detected in the x-ray diffraction patterns.

The neutron scattering experiments in the temperature range of 1.6 – 100 K were performed on the cold neutron powder diffractometer DMC [28] at Swiss spallation neutron source SINQ [29]. The sample was enclosed in a cylindrical vanadium container under helium atmosphere and mounted in a helium cryostat. The neutron wavelength used was $\lambda = 2.4576$ Å. The data has been corrected for absorption and was refined using the FULLPROF program package [30]. For the refinement of the magnetic structure at 1.6 K the paramagnetic data at 30 K was subtracted to obtain the pure magnetic diffraction pattern.

Experimental results and their discussion

We measured the temperature dependence of the specific heat $C_p(T)$ between 2 and 300 K and the magnetic field 0 and 9 T [13]. The calorimetric investigations in the temperature range of 2–300 K in magnetic fields up to 9 T were performed using a Quantum Design PPMS 6000 instrument at Krasnoyarsk Shared Usage Scientific Center.

The temperature dependence of the $\text{NaFeGe}_2\text{O}_6$ specific heat in the absence of the external magnetic field ($H=0$) exhibits a sharp maxima at the temperatures $T_1 = 11.6$ K and $T_2 = 13$ K (fig. 2). There are two phase transitions in this clinopyroxene-type $\text{NaFeGe}_2\text{O}_6$ compound at $H=0$. The position of the first maximum ($T_1 = 11.6$ K) in the $C_p(T)$ curve depends on magnetic field. The position of the second maximum ($T_2 = 13$ K) is not depend on magnetic field range of 0–9 T.

Also the magnetic susceptibility measurements had showed that the magnetic structure modification takes place near temperature $T_1 = 11.6$ K [13].

Using neutron powder diffraction the magnetic order below $T_N \approx 13$ K was confirmed again in the $\text{NaFeGe}_2\text{O}_6$ [31, 32]. The fig. 3 shows the temperature dependence of the integrated intensity of the strongest magnetic peak $(0, 0, 0) \pm k$ in the diffraction pattern of the neutron magnetic scattering in the $\text{NaFeGe}_2\text{O}_6$. This magnetic peak does not overlap with any other peaks and the fit program can easily determine the intensity. The phase transition which take a place in the $\text{NaFeGe}_2\text{O}_6$ and is shown on the temperature dependence of the specific heat at $T_2 = 13$ K (fig. 2) corresponds to the transition from paramagnetic to antiferromagnetic state, so $T_2 = T_N = 13$ K. The temperature of the magnetic ordering T_N is low due to the competition between the intra- and interlayer exchange interactions of chains which were analyzed in [11].

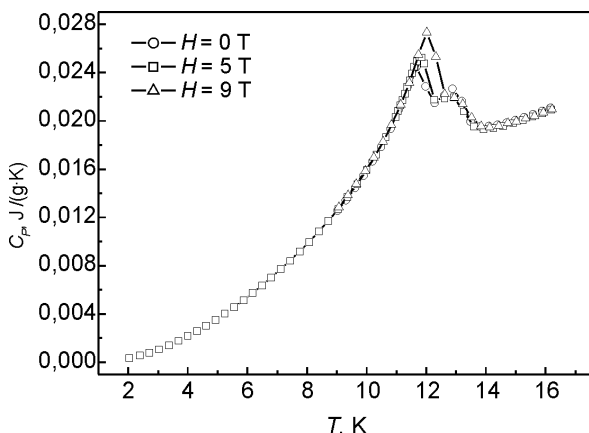


Fig. 2. Temperature dependence of the specific heat of $\text{NaFeGe}_2\text{O}_6$ in magnetic field $H = 0, 5, 9$ T.

Table 2

The neutron scattering results for $\text{NaFeGe}_2\text{O}_6$ spin arrangement at 1.6 K

Propagation vector	$\mathbf{k} = (0.3357(4), 0, 0.0814(3))$
Moment arrangement:	helical modulation of antiferromagnetically coupled pairs
The ordered moment per Fe^{3+} ion	$M = 2.55(1) \mu_B$
Plane of moments	close to $a-c$ plane (small component along b)
Reliability factors of refinement	$R_p = 4.5, \chi^2 = 4.43$

Neutron powder diffraction experiments ($\lambda = 2.4576 \text{ \AA}$) results in $\text{NaFeGe}_2\text{O}_6$ magnetic structure study are listed in table 2. The magnetic structure wave vector $\mathbf{k} = (0.3357(4), 0, 0.0814(3))$ at 1.6 K.

On the basis of neutron diffraction measurements we concluded that the $\text{NaFeGe}_2\text{O}_6$ magnetic structure is incommensurate and consists of antiferromagnetically coupled Fe^{3+} pairs with helical modulation within the $a-c$ plane of the crystal lattice (fig. 3). The $\text{NaFeGe}_2\text{O}_6$

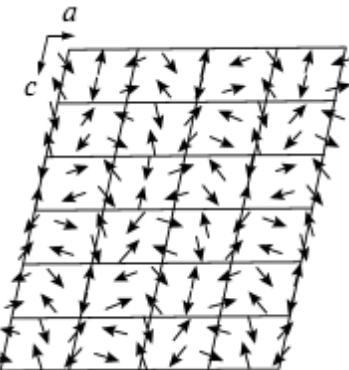


Fig. 3. Magnetic structure below $T_1 = 11.6$ K in $\text{NaFeGe}_2\text{O}_6$.

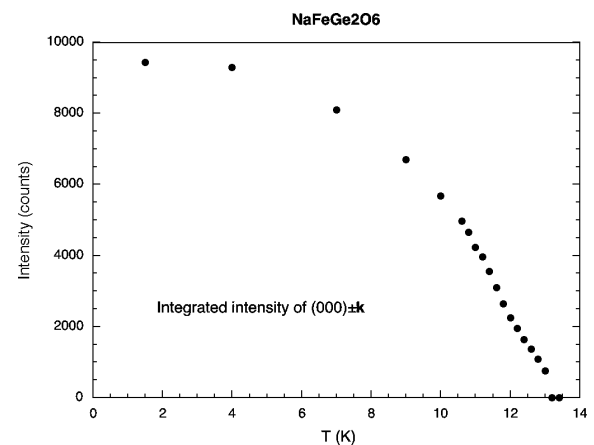


Fig. 4. Temperature dependence of the integrated intensity of the Bragg magnetic peak $(0, 0, 0) \pm k$ on the $\text{NaFeGe}_2\text{O}_6$ neutron diffraction pattern. The Neel temperature is $T_N = 13$ K.

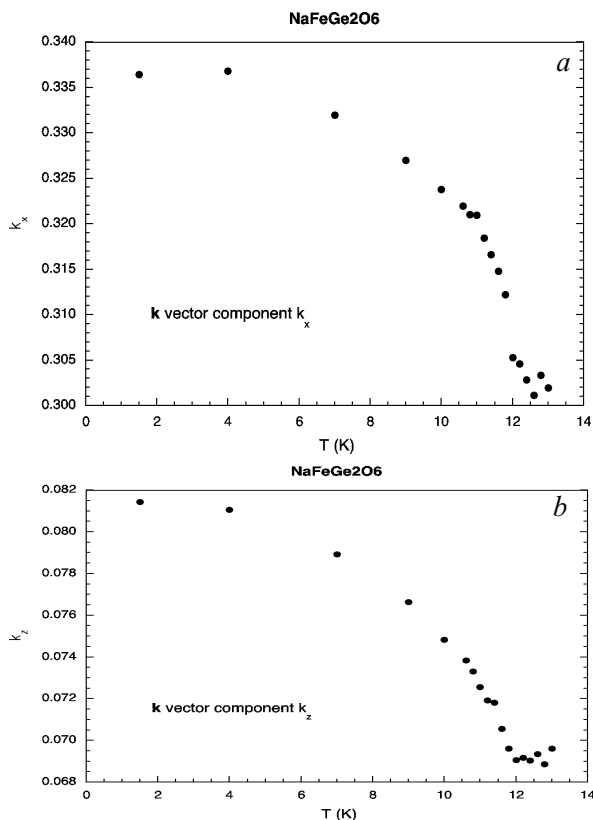


Fig. 5. Temperature dependence of the wave vectors k_x (a) and k_z (b) of the magnetic structure for $\text{NaFeGe}_2\text{O}_6$.

helical magnetic structure is apparently due to the “competition” of exchange interactions of different atomic neighbors of Fe^{3+} ions [33].

This magnetic structure is the same up to 11.6 K. In the integrated intensity curve there is a change of slope at 12 K, indicating the second phase transition (fig. 4).

The fig. 5 shows components of the \mathbf{k} vector: the component k_x (fig. 5a) and the component k_z (fig. 5b). The temperature dependence of k_x and k_z also show two phase transitions. Between 13 and 12 K the components of k are slowly changing. At 12 K both components start to increase quite steeply and then settle at the low temperature values at 1.6 K. The evolution of the \mathbf{k} vector was determined only by use of the magnetic peak positions and no magnetic model was involved.

It is not possible to refine a full magnetic model at magnetic field $H = 0$ because the magnetic intensities are too small in the reason of the experimental data close to the ordering temperature T_N . There are no dramatic changes of relative intensities of different magnetic peaks above and below 12 K. So we may conclude that the two magnetic phases must be closely related.

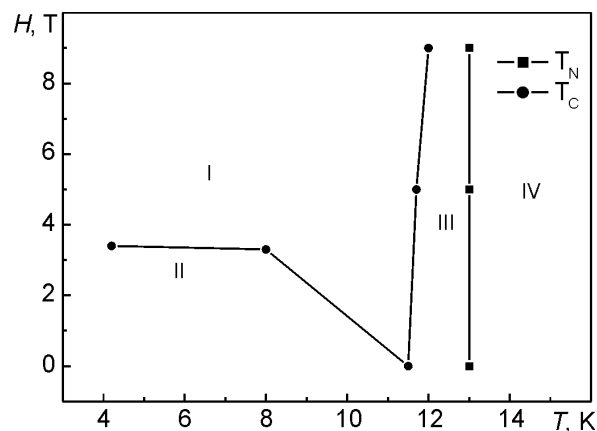


Fig. 6. Phase diagram of the magnetic state in $\text{NaFeGe}_2\text{O}_6$. Magnetic structure is incommensurate in region II and paramagnetic in region IV. It is unknown in regions I and III.

On the basis of the experimental data of the compound $\text{NaFeGe}_2\text{O}_6$ we plot the phase diagram of the magnetic state (fig. 6). Magnetic structure is incommensurate in region II and paramagnetic in region IV. It is unknown in regions I and III.

Conclusion

The magnetic structure and phase transitions of the sodium iron germanate $\text{NaFeGe}_2\text{O}_6$ was studied by neutron diffraction.

In summary we conclude that the neutron diffraction results are in a good agreement with the data of the specific heat measurements. There are clear changes in the temperature dependence of the integrated intensity curve at 12 K indicating two ordered magnetic phases in zero magnetic field.

Below $T_N \approx 13$ K the compound $\text{NaFeGe}_2\text{O}_6$ undergoes a phase transition disorder — order (from the paramagnetic state to antiferromagnetic state).

The magnetic structure of $\text{NaFeGe}_2\text{O}_6$ is not determined in the temperature range $11.6 \text{ K} > T > 13 \text{ K}$ and the magnetic field $H = 0$. It is not possible to refine by the neutron diffraction experiment because the magnetic intensities are too small.

Below $T_1 = 11.6$ K the magnetic structure undergoes to an incommensurate structure. Antiferromagnetically coupled pairs of Fe^{3+} moments show an helical modulation according to the magnetic propagation vector \mathbf{k} within the ac plane and no modulation along b .

Neutron beam time at the cold neutron powder diffractometer DMC at the Swiss spallation neutron source SINQ, Paul Scherrer Institute, Villigen, Switzerland is gratefully acknowledged.

Literature

1. Streltsov S.V., Khomskii D.I. Electronic structure and magnetic properties of pyroxenes (La, Na)TM(Si, Ge)₂O₆: Low-dimensional magnets with 90° bonds. *Phys. Rev.*, 2008, B 77, p. 064405-1 – 064405-11.
2. Katanin A.A., Irhin V.Yu. Magnetic order and spin fluctuation in low-dimensional system. *Uspekhi Fiz. Nauk* 2007, v. 177, p. 639 – 662.
3. Jodlauk S., Becker P., Mydosh J.A., Khomskii D.I., Lorenz T., Streltsov S.V., Hezel D.C., Bohaty L. Pyroxenes: a new class of multiferroics. *J. Phys. Cond. Matter*. 2007, v. 19, p. 432201 – 432210.
4. Vasiliev A.N., Ignatchik O.L., Isobe M., Ueda Y. Long range Neel order in quasi-one-dimensional vanadium-based ($s=1$) pyroxenes (Li, Na)V(Si, Ge)₂O₆. *Phys. Rev.* 2004, B 70, p. 132415-1 – 132415-4.
5. Emirdag-Eanes Mehtap, Kolis Joseph W. Hydrothermal synthesis, characterization and magnetic properties of NaVGe₂O₆ and LiVGe₂O₆. *Mater. Research Bull.* 2004, v. 39, p. 1557 – 1567.
6. Mila F., Zhang F.C. On the origin of biquadratic exchange in spin 1 chain. *Eur. Phys. J.* 2000, B16, p. 7 – 10.
7. Millet P., Mila F., Zhang F.C., Mambrini M., Van Oosten A.B., Pashchenko V.A., Sulpice A., Stepanov A. Biquadratic interactions and spin-Peierls transition in spin-1 chain LiVGe₂O₆. *Phys. Rev. Lett.* 1999, v. 83, p. 4176 – 4179.
8. Redhammer G.J., Roth G., Treutmann W., Hoelzel M., Paulus W., Andre G., Pietzonka C., G. Amthauer. The magnetic structure of clinopyroxenes-type LiFeGe₂O₆ and revised data on multiferroic LiFeSi₂O₆. *J. Solid State Chem.* 2009, v. 182, p. 2374 – 2384.
9. Redhammer G.J., Roth G., Paulus W., Andre G., Lottermoser W., Amthauer G., Treutmann W. The crystal and magnetic structure of Li-aegirine LiFe₃⁺Si₂O₆: temperature-dependent study. *Phys. Chem. Minerals*, 2001, v. 28, p. 337 – 346.
10. Drokina T.V., Petrakovskii G.A., Bayukov O.A., Bovina A.F., Shimchak R., Velikanov D.A., Kartashev A.V., Volkova A.L., Ivanov D.A., Stepanov G.N. Properties of clinopyroxene LiFeGe₂O₆. *Phys. Solid State*, 2010, v. 52, p. 2250 – 2253.
11. Drokina T.V., Bayukov O.A., Petrakovskii G.A., Velikanov D.A., Bovina A.F., Stepanov G.N., Ivanov D.A. Synthesis and properties of NaFeGe₂O₆. *Phys. Solid State*, 2008, v. 50, p. 2141 – 2144.
12. Drokina T., Petrakovskii G., Keller L., Schefer J., Ivanov D. Magnetic structure and properties of pyroxene NaFeGe₂O₆. *China. Rare Metals*, 2009, v. 28, p. 398 – 400.
13. Drokina T.V., Petrakovskii G.A., Keller L., Schefer J., Balaev A.D., Kartashev A.V., Ivanov D.A. Modulated magnetic structure in quasi-one-dimensional clinopyroxene NaFeGe₂O₆. *JETP* 2011, v. 112, p. 121 – 126.
14. Redhammer G.J., Senyshyn A., Meven M., Roth G., Prinz S., Pachler A., Tippelt G., Pietzonka C., Treutmann W., Hoelzel M., Pedersen B., Amthauer G. Nuclear and incommensurate magnetic structure of NaFeGe₂O₆ between 5 K and 298 K and new date on multiferroic NaFeSi₂O₆. *Phys. Chem. Minerals* 2010, DOI 10.1007/s00269-010-0390-3 (Springer).
15. Baum E., Treutmann W., Behruzi M., Lottermoser W., Amthauer G. Structural and magnetic properties of the clinopyroxenes NaFeSi₂O₆ and LiFeSi₂O₆. *Zeitsch. Fur Kristal.* 1988, v. 183, p. 273 – 284.
16. Baker P.J., Lewtas H.J., Blundell S.J., Lancaster T., Franke I., Hayes W. Pratt F.L., Bohary L., Becker P. Muon-spin relaxation and heat capacity measurements on the magnetoelectric and multiferroic pyroxenes LiFeSi₂O₆ and NaFeSi₂O₆. *Phys. Rev.* 2005, B 81, p. 214403-1 – 214403-5.
17. Vasiliev A.N., Ignatchik O.L., Sokolov A.N., Hiroi Z., Isobe M., Ueda Y. Long-range magnetic order in quasi-one-dimensional chromium-based ($s=3/2$) pyroxenes (Li, Na)Cr (Si, Ge)₂O₆. *Phys. Rev.*, 2005, B 72, p. 012412-1 – 012412-4.
18. Vasiliev A.N., Ignatchik O.L., Sokolov A.N., Hiroi Z., Isobe M., Ueda Y. Long-range magnetic order in quasi-one-dimensional oxides NaCrSi₂O₆ and NaCrGe₂O₆. *JETP Letters*, 2003, v. 78, p. 1039 – 1042.
19. Nenert G., Ritter C., Isobe M., Isnard O., Vasiliev A.N., Ueda Y. Magnetic and crystal structures of the one-dimensional ferromagnetic chain pyroxene NaCrGe₂O₆. *Phys. Rev.* 2009, B 80, p. 024402-1 – 024402-7.
20. Nenert G., Kim I., Isobe M., Ritter C., Vasiliev A.N., Kim K.H., Ueda Y. Magnetic and magnetoelectric study of the pyroxene NaCrSi₂O₆. *Phys. Rev.* 2010, B 81, p. 184408-1 – 184408-4.
21. Isobe M., Ninomiya E., Vasiliev A.N., Ueda Y. Novel Phase Transition in Spin-1/2 Linear Chain Systems: NaTiSi₂O₆ and LiTiSi₂O₆. *J. Phys. Soc. Jpn.* 2002, v. 71, p. 1848 – 1851.
22. Popović Z.S., Điljančanin P.V., Vukajlović Filip R. Sodium pyroxene NaTiSi₂O₆: possible haldane spin-1 chain system. *Phys. Rev. Lett.* 2004, v. 93, p. 036401-1 – 036401-4.
23. Sasago Y., Hase M., Ushinokura K., Tokunaga M., Miura N. Discovery of spin-singlet ground state with an energy gap in CaCuGe₂O₆. *Phys. Rev.* 1995, B 52, p. 3533 – 3539.
24. Coey J.M.D., Ghose S. Magnetic order in hedenbergite: CaFe²⁺Si₂O₆. *Solid State Commun.* 1985, v. 53, p. 143 – 145.
25. Redhammer G.J., Roth G., Treutman W., Paulus W., Andre G., Pietzonka C., Amthauer G. Magnetic ordering and spin structure in Ca-bearing clinopyroxenes CaM²⁺(Si, Ge)₂O₆, M=Fe, Ni, Co, Mn. *J. Solid State Chem.*, 2008, v. 18, p. 13163 – 13176.
26. Durand G., Vilminot S., Rabu A., Derory A., Lamboour J.P., Ressouche E. Synthesis, structure, and magnetic properties of CaMSi₂O₆ (M = Co, Ni) compounds and their solid solutions. *J. Solid State Chem.*, 1996, v. 124, p. 374 – 378.
27. Solovyova L.P. and Bakakin V.V. X-ray investigation of Na, Fe-metagermanate NaFeGe₂O₆. *Krystallographiya*, 1967, v. 12, p. 591 – 594.
28. Fischer P., Keller L., Scheffler J., Kohlbrecher J. Neutron diffraction at SINQ. *Neutron News* 2000, v. 11, p. 19 – 21.
29. Fischer W.E. SINQ - The spallation neutron source, a new research facility at PSI. *Physica*, 1997, B 234 – 236, p. 1202 – 1208.

33. Rodriguez-Cravalal Recent Advances in Magnetic Structure Determination by Neutron Powder Diffraction. *J Physica B: Condens. Matter.* 1993, v. 192, p. 55 – 69.
31. Drokina T., Petrakovskii G., Keller L., Schefer J. Investigation of the magnetic structure in $\text{NaFeGe}_2\text{O}_6$ using neutron powder diffraction. *Journal of Physics: Conference Series.* 2010, v. 251, p. 012016 – 012020.
32. Schefer J., Keller L., Drokina T., Petrakovskii G. Incommensurate magnetic structure of $\text{NaFeGe}_2\text{O}_6$ pyroxene investigated by neutron powder diffraction. Thesis. International conference on Newtron Scattering (ICNS 2009). 3 – 7 May, 2009. Knoxville, Tennessee, USA.
33. Izumov Yu.A. *Diffraction of Neutrons on Long-Period structures* 1987, (Energoatomizdat, Moscow), 200 p.

Дрокина Тамара Васильевна — Институт физики им. Л.В. Киренского Сибирского отделения Российской академии наук (г. Красноярск), кандидат физико-математических наук, старший научный сотрудник. Специалист в области физики магнитных явлений. E-mail: tvd@iph.krasn.ru.

Петраковский Герман Антонович — Институт физики им. Л.В. Киренского Сибирского отделения Российской академии наук (г. Красноярск), Заслуженный деятель науки, доктор физико-математических наук, главный научный сотрудник. Специалист в области физики магнитных явлений. E-mail: gap@iph.krasn.ru.

Келлер Л. — Институт им. Пауля Шеррера, лаборатория нейтронного рассеяния, WHGA-244, CH-5232 (Виллиген, Швейцария).

Шефер Й. — Институт им. Пауля Шеррера, лаборатория нейтронного рассеяния, WHGA-244, CH-5232 (Виллиген, Швейцария).